Journal of King Saud University - Science 36 (2024) 103167

HOSTED BY

Contents lists available at ScienceDirect

Journal of King Saud University - Science

journal homepage: www.sciencedirect.com

Full Length Article

Potential of recycled polypropylene: A study on effect of natural fiber on the morphology and properties of biocomposite

Abdulmohsen Albedah [a,*], Hany S. Abdo [b], Sohail M.A.K. Mohammed [c], Bel Abbes Bachir Bouiadjra [a,d], Ebrahim H. Al-Ghurabi [e], Othman Y. Alothman [e]

[a] Mechanical Engineering Department, College of Engineering, King Saud University, Riyadh 11421, Saudi Arabia
[b] Centre of Excellence for Research in Engineering Materials, Deanship of Scientific Research, King Saud University, Riyadh 11421, Saudi Arabia
[c] Department of Mechanical and Materials Engineering, Florida International University, 10555 West Flagler Street, Miami, FL 33174, USA
[d] LMPM, Department of Mechanical Engineering, University of Sidi Bel Abbes, BP 89, Cité Ben M'hidi, Sidi Bel Abbes 22000, Algeria
[e] Department of Chemical Engineering, College of Engineering, King Saud University, Riyadh, Saudi Arabia

ARTICLE INFO

Keywords:
Date palm fiber
Recycled-Polypropylene
Biocomposite
Mechanical Properties

ABSTRACT

This research explores the innovative fabrication and characterization of recycled polypropylene composites that reinforced by natural fibers, specifically date palm micro fibers (DPF). Employed a twin-screw extruder for the mixing, and injection molding technique for the samples fabrication. DPF was incorporated at varying weight percentages (0, 2, 5, and 10 wt%). A comprehensive analysis, including thermal gravimetric analysis (TGA), Fourier-transform infrared spectroscopy (FTIR) and X-ray diffraction (XRD), was conducted to assess thermal stability, chemical interactions and crystalline structure. Mechanical properties were evaluated through shore-D hardness and uniaxial tensile tests. Notably, the study revealed that an increased DPF filler content resulted in superior mechanical properties, such as enhanced shore-D hardness and tensile strength. This improvement was attributed to the alignment of DPF fillers and the recycled polypropylene matrix. The significance of this research lies in showcasing the promising potential of DPF as an eco-friendly reinforcement material in recycled polypropylene biocomposites, providing a sustainable and environmentally friendly alternative for various engineering applications. The work contributes to advancing greener solutions in material science and highlights the unique advantages of DPF in enhancing composite materials.

1. Introduction

In recent years, there has been a growing interest in exploring sustainable materials for various engineering applications to mitigate environmental concerns and promote a circular economy. One such promising area is the incorporation of natural fibers into polymer matrices to create eco-friendly and lightweight composites (Mary Jasmin et al., 2023; Sahu et al., 2023; Sathish et al., 2023). These materials possess biodegradability and are recognized for their eco-friendliness in various industrial applications. Among the diverse range of natural fibers, date palm fibers (DPFs) have gained considerable attention due to their abundance, low cost, and remarkable mechanical properties. DPF belongs to the palm tree family (*phoenix dactylifera*), can grow for more than 100 years, and is abundantly found in the world. Nevertheless, a challenge that has persisted in natural fiber reinforced biopolymer composites is the issue of incompatibility at the interface in the dichotomy between the hydrophilic characteristics inherent to natural fibers and the hydrophobic attributes exhibited by polymer matrices (Ali et al., 2018; Fouly et al., 2021; Shaikh et al., 2023). However, the tensile strength of DPFs is moderate and can range from 58 to 203 MPa, but possess considerable ductility of up to 10 % (Adamu et al., 2023; Al-Khanbashi et al., 2005; Alawar et al., 2009). In addition, the elastic modulus of the natural fibers are equivalent and sometimes higher than glass fibers (Saheb and Jog, 1999). Hence can be a potential reinforcement for polymer composites with moderate or high load carrying applications.

Polymers, including polyolefins, are usually used as matrices to fabricate composites due to their versatile behavior (Ahmad et al., 2023; Bouakkaz et al., 2018; Singh et al., 2023). One of the most widely used polyolefins is polypropylene, as a result of its availability and durability with high stiffness, good chemical stability, low density, and excellent thermal resistance (Ku et al., 2011; Sarmin et al., 2023). However, due

* Corresponding author. Tel.: +966-114676827; fax: +966-114677339.
E-mail address: albedah@ksu.edu.sa (A. Albedah).

https://doi.org/10.1016/j.jksus.2024.103167
Received 21 November 2023; Received in revised form 7 January 2024; Accepted 14 March 2024
Available online 15 March 2024

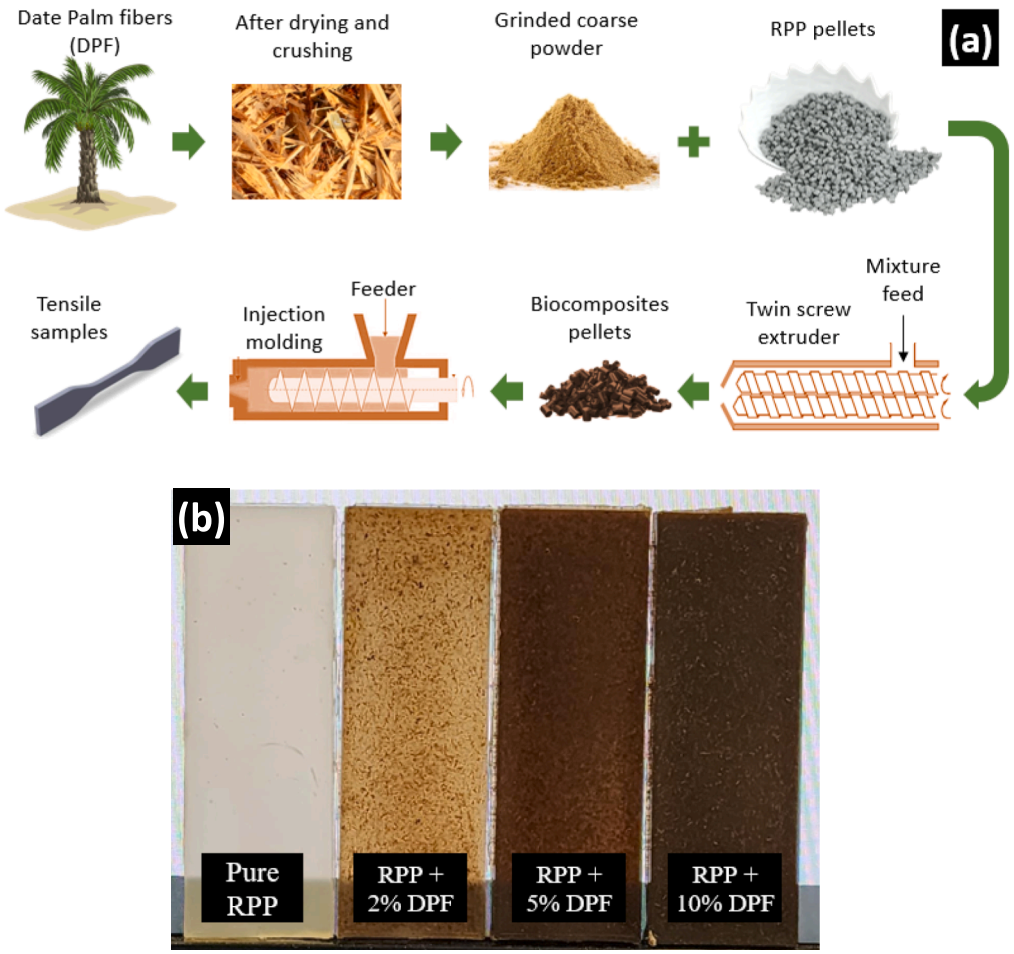

Fig. 1. (a) Schematic diagram for the fabrication process, (b) fabricated biocomposites samples showing a homogeneous distribution of the DPF fillers.

to awareness of plastics impact on environment and subsequent regulations regarding pollution control, recycling of polymers, including polypropylene, has been under extensive investigation (Al-Otaibi et al., 2020; Alzebdeh et al., 2021; Gideon and Atalie, 2022; Islam et al., 2014; Kusuma et al., 2021; Zadeh et al., 2017). Recycled polypropylene (rPP) has thus attracted several industries including automotives where at least 25 % of the recycled plastic would be used in the automotives by the year 2025 (Chiang et al., 2020; Ladhari et al., 2021). However, for recycled plastics to serve as a viable substitute, recyclers must ensure that they meet the necessary technical and quality standards, surpassing those of the virgin material. (Rahimi and García, 2017). As such, Islam *et al.* (Islam et al., 2014) investigated the effect of alkali-treatment on the morphological and mechanical properties of kenaf/rPP composites. Elke and Wichman (Selke and Wichman, 2004) explored the impact and tensile strength of high-density polyethylene reinforced with wood and paper fibers from post-consumer sources. Their findings indicated that the inclusion of wood fibers has a tendency to enhance impact strength, although it has a diminishing effect on elongation at break. Al-Otaibi *et al.* (Al-Otaibi et al., 2020) investigated date palm fiber composites with three different PP types including rPP, focusing on the treatment effect on DPF. Zadeh *et al.* (Zadeh et al., 2017) studied flammability of recycled PP/LDPE/HDPE blend filled with DPF. Hoang *et al.* (Quynh Truong Hoang et al., 2010) used recycled polypropylene which was recycled mechanically 10 times and reinforced with spruce fibers. Although the tensile strength decreased in the composite, the reinforcement of spruce fibers compensated for the degradation of stiffness due to recycling. Potential benefits of using recycled composite were highlighted in the study. The present study also emphasized the feasibility of using recycled PP as a potential matrix for making a natural composite. Starting from recycling the post-consumer PP to making its composite followed by extensive thermo-mechanical characterization is the highlight of current study. The current work not only explores the enhancements in mechanical properties but also delves deep into the underlying thermal and chemical aspects through TGA, XRD, and FTIR analyses.

In this study, sustainable biocomposite is successfully fabricated by reinforcing DPF with recycled Polypropylene using injection molding technique. The study delves into extensive thermal and mechanical characterization of biocomposite to elucidate their usage in practical applications. Thermal gravimetric analysis (TGA), Fourier-transform IR spectroscopy (FTIR) and XRD, were carried out to assess thermal stability, chemical interactions, and crystalline structure, besides uniaxial tension test to evaluate the mechanical behavior. The findings presented herein will contribute to the advancement of eco-friendly materials and support the transition towards a greener and more sustainable future.

2. Materials and methods

Recycled polypropylene (rPP) (Saudi Top Plastic Trading Company, Saudi Arabia) was used as the matrix. The melt flow index (MFI) in as-received condition was ~ 0.655 g/min. DPF were used as secondary fillers. The fronds of date palm were collected from local farms followed by washing by purified water and drying under sun for 48 h to ensure removal of any moisture content. The dried fronds were then ground to obtain DPF followed by sieving on sizes ranging from 425 to 600 μm.

2.1. Fabrication of biocomposites

The rPP was mixed with DPFs with different compositions (2, 5 and 10 wt%). As described in the schematic in Fig. 1a, they were first pre-mixed using a mechanical mixer to disperse the DPF into the rPP matrix. Subsequently, the pre-blended raw materials underwent extrusion at a constant temperature spanning ten different zones from 160 °C up to 210 °C, operating at a rotational speed of 50 rpm, resulting in the formation of a wire. This strand was subsequently processed through a pelletizer to generate pellets. The twin-screw extruder in the present study had a 16 mm screw diameter which resulting in a L/D ratio of 40. The composite pellets were later fed into an injection molding machine with three different temperature zones of 180 °C, 195 °C, and 220 °C to produce the different testing samples of the rPP/DPF composite shown in Fig. 1b.

2.2. Characterization

Melt flow index (MFI) is a commonly used method in the plastics industry to characterize the viscosity of thermoplastic materials. It allows to estimate their extrudability. Flow behaviors of samples was determined using a load of 2.16 kg at 230 °C. The MFI was measured according to the ISO 1133 standard. The MFI of recycled PP was evaluated to ensure the quality of rPP in comparison with the commercial PP. X-ray pattern of the raw fibers were obtained by an X-ray diffractometer (XRD) D-8 Discover, Bruker, Germany. The setup comprises a rotary anode generator featuring a copper target and a broad-angle powder goniometer. The XRD was performed in the 2θ range of 5–90°at 40 kV, using a filtered Cu Kα radiation utilizing a wavelength (λ) of 1.5406 Å and 40 mA current.

Thermal analysis was performed using an SDT Q600 setup (TA Instruments, USA) with a nitrogen purge gas. Approximately 10–15 mg of the specimen was utilized for each measurement. The samples underwent heating from room temperature (25 °C) to 800 °C at a rate of 10 °C/min. A consistent flow of nitrogen gas at 90 mL/min was maintained throughout the experiment. Fourier transform infrared spectroscopy (FTIR) investigations were conducted using a Bruker TENSOR Series FT-IR spectrophotometer from Germany. Spectra were recorded in the range of 4500 to 600 cm-1, with 4 cm-1resolution, and 32 scans in average. Hardness tests were curried out utilizing Durometer according to ASTM D2240-15 type D (Shore-D). The readings were taken 1 s after the needle is brought in contact with the sample. At least five measurements were performed for each sample.

Uniaxial tensile experiments were performed on a universal testing machine of 150 kN (Instron ElectroPuls E10000, Norwood, MA) following ASTM D638 standard. The dog-bone shape tensile specimen had a gauge length of 70 mm, gauge width and thickness of 12 and 2 mm, respectively. The experiments were carried out at room temperature with an average speed of 5 mm/min for all samples. The yield strength (YS), ultimate tensile strength (UTS) and elongation at break were calculated from the data. The tensile tests were performed on more than three samples for each composition.

3. Results and discussion

3.1. Effect of DPF on crystallinity

Prior to crystallinity, the rPP samples were tested for MFI to ensure their quality compared to commercial PP. The average MFI of rPP was found to be 7.2 g/10 min which is in comparison with the existing literature and slightly higher. The MFI of rPP increases slightly with recycling due to the presence of foreign particles like polyethylene as commonly reported (Ferg and Bolo, 2013). X-ray diffraction was employed to examine the physical structural alterations of the fibers, specifically in terms of crystallinity index (CI). Segal *et al.* (Segal et al., 1959) have developed an empirical method to estimate the crystallinity

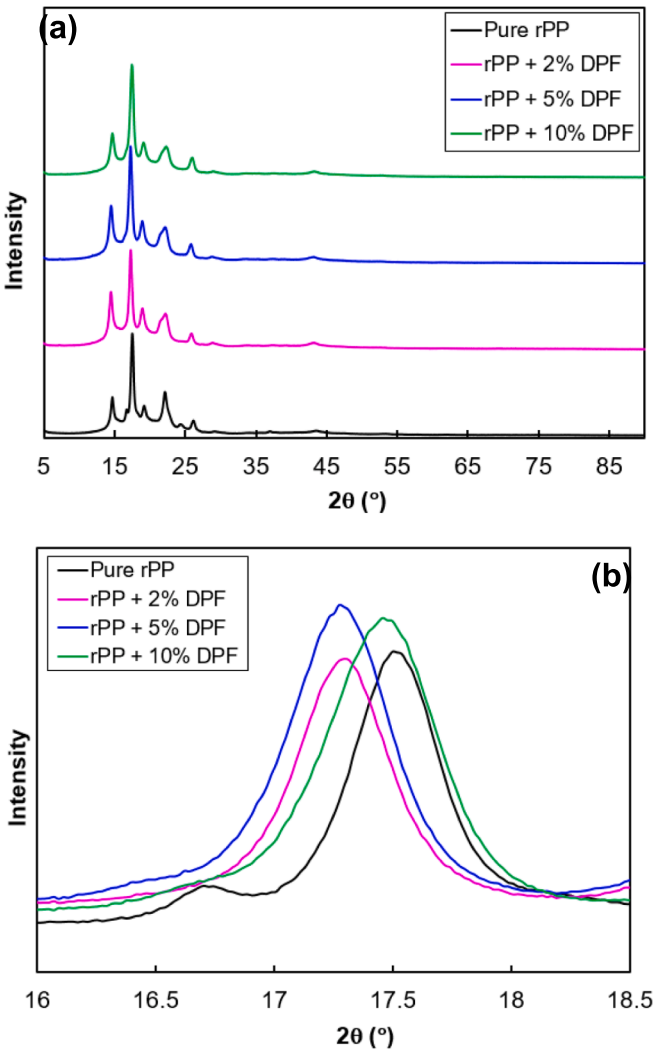

Fig. 2. (a) XRD patterns of rPP and DPF/rPP composites (b) major peak shifting of the XRD patterns for rPP and DPF/rPP composites.

index:

$$CI\% = \frac{I_{002} - I_{am}}{I_{am}} \times 100 \quad (1)$$

where I_{002} represents the intensity of (0 0 2) at a diffraction peak of $2\theta = 17.5^{\circ}$ for cellulose I i.e., native cellulose, and I_{am} signifies the intensity scattered by the amorphous region of the sample. The corresponding intensity is the minimum which is about $2\theta = 15^{\circ}$. The crystallinity of as received DPF is also measured which is evaluated to be 2.6 nm and the corresponding CI is 66.3 %.

The XRD analysis of rPP/DPF composites in Fig. 2(a) shows peak shifting, where the positions of the main diffraction peaks in the X pattern of the composite are different compared to the neat rPP. This peak shifting can occur due to the changing of degrees of crystallinity, where higher crystallite size corresponds to lower degree of crystallinity and vice versa. In XRD analysis, microstrain and crystallite size are related through the Williamson-Hall equation. This equation evaluates the broadening of diffraction peaks in the XRD pattern due to the presence of microstrain and finite crystallite.

The Williamson-Hall equation is as follows:

$$\beta\cos\theta = \frac{k\lambda}{D} + 4\varepsilon\sin\theta \quad (2)$$

In this equation, β denotes the full width of the diffraction peak at its half

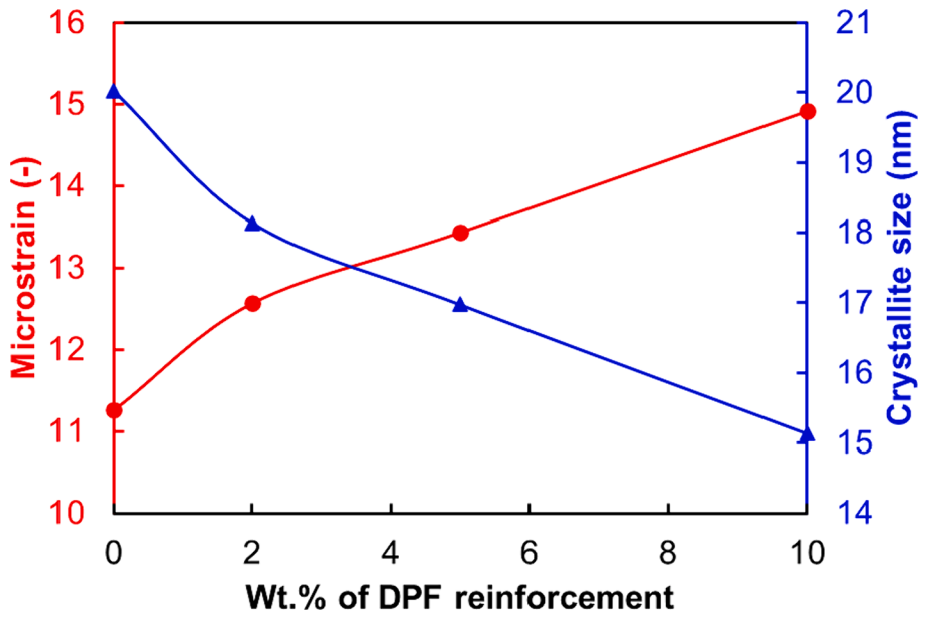

Fig. 3. Microstrain and crystallite size of DPF reinforced rPP with varying fraction of DPFs.

Table 1
Crystallite size values calculated for the major peak of each composite.

Fiber Fraction (%)	2θ (°)	FWHM	D (nm)	β × 10^{-3} (nm^{-2})	ε×10^{-3}
0	17.495	0.397	20.02	2.49	11.26
2	17.291	0.438	18.14	3.04	12.57
5	17.283	0.468	16.98	3.47	13.44
10	17.461	0.525	15.14	4.36	14.92

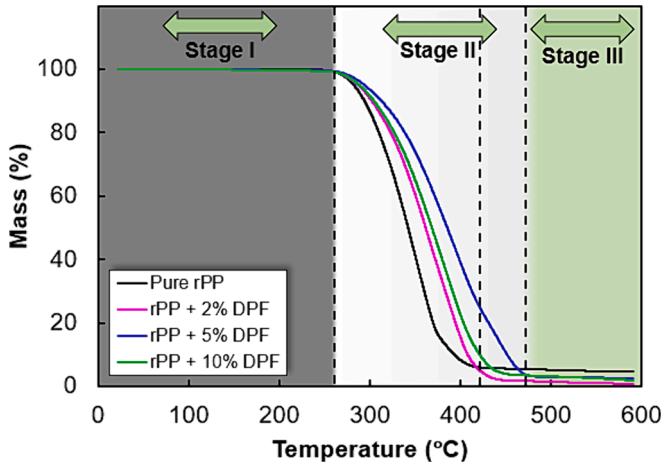

Fig. 4. TGA curves of rPP and DPF/rPP composites.

maximum (FWHM), θ represents the Bragg angle, and K is the shape factor, often assumed to have a typical value of 0.9, λ is the X-ray radiation wavelength, and ε is the microstrain. The term $K\lambda$ represents the broadening of the diffraction peak due to the finite size of the crystallites. As the crystallite size decreases, the peak broadens, resulting in a larger β value. The term $4\varepsilon sin\theta$ represents broadening of the diffraction peak due to the presence of microstrain. Microstrain refers to local lattice distortions or defects within the crystallites, causing the ideal positions and leading to peak broadening. As the microstrain increases, the peak broadens, resulting in a higher β value. Fig. 3 and Table 1 present the crystallite size and microstrain values for the different composite samples, providing an estimation of the degree of crystallinity in the crystalline phase. It is evident from the Fig. 3 that the of crystallinity increases as the DPF content in the fabricated composites increases.

The increased crystallinity index of the fabricated composites as the percentage of DPF increases indicates enhancement in the form of hydrogen bonds between cellulose chains. Consequently, the chemical bonding between the fibers increases.

3.2. *Thermal properties*

The degradation properties of the materials fabricated were evaluated with respect to morphological, thermal, and mechanical variation of the composites. The thermal degradation properties were compared by means of TGA tests as shown in Fig. 4. In general, thermal degradation of the DPF-reinforced composites consisted of three degradation stages – first stage was observed below 280 °C where, the slight weight loss of the rPP/DPF specimens mainly resulted from the loss of moisture inside the specimens, while no loss was observed for the unfilled rPP. The second stage appeared at temperatures between 280 and 420 °C in rPP, whereas it was 280–460 °C in the DPF-reinforced composites. The second stage naturally exhibited largest weight loss attributed to degradation of the microstructural component of the composite. As expected, the rPP degradation temperature range (280–420 °C) is less than that of reported virgin PP, which is around (300–475 °C) (Esmizadeh et al., 2020), as a result of thermal history of reprocessing. In case of rPP/DPF composites the presence of lignin, hemicellulose, etc. exhibits various degradation temperatures. While the lignin content has not been quantified in the current study, it is important to note that DPF inherently contain lignin. Consequently, as the DPF loading increases in the composite, the overall lignin percentage in the material will automatically rise. This can contribute to an elevation in the composite's degradation temperature, given the generally higher degradation temperature associated with lignin. The study emphasizes the implicit influence of DPF, including its lignin content, on the thermal behavior of the composite, suggesting a potential avenue for further investigation into the specific role of lignin in enhancing thermal stability.. The final stage of weight loss beyond 460 °C could be neglected due to minor changes in the weight loss (<5%). As the DPF fraction increases, the thermal degradation temperature increases. This could be attributed to the fiber retardation of the free radicals due to rPP degradation (Mofokeng et al., 2012). However, the composite with 10 % DPF exhibited

Table 2
DSC data of the rPP and DPF/rPP composites.

Fiber Fraction (%)	T_m °C	ΔH_m (J/g)	T_c °C	X_c (%)
0	163.82	63.06	115.21	30.17
2	162.48	79.70	111.37	38.52
5	161.05	83.82	116.14	40.92
10	161.83	71.44	116.24	35.24

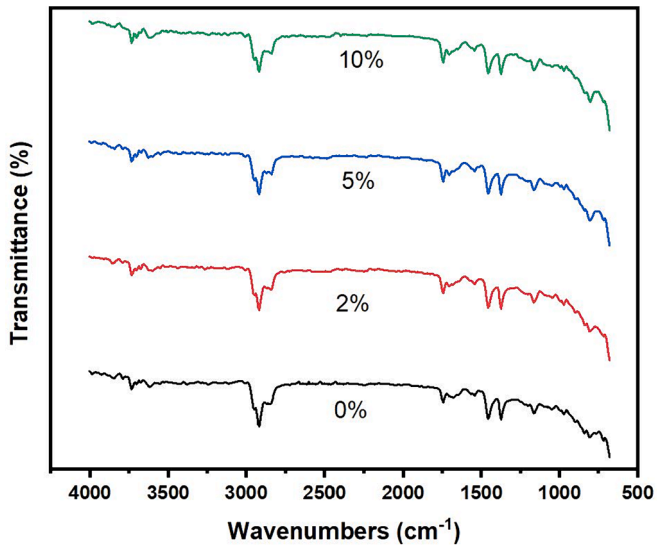

Fig. 5. FTIR spectra of rPP and DPF/rPP composites.

earlier degradation compared to 5 % DPF composite, yet later than the 2 % DPF composite. This could be attributed to formation of agglomerates due to higher volume fraction of DPF.

Table 2 shows the thermal properties of pure rPP and DPF/rPP fabricated composites obtained using differential scanning calorimetry (DSC). While little differences in the melting and crystallization temperatures were observed, an increase of up to 33 % can be seen at composite with 5 % DPF.

Fig. 5 shows the FTIR spectra of the rPP/DPF composites. Overall, there is no evident difference in the FTIR spectra of rPP and DPF/rPP composite. The lack of discernible differences in the FTIR spectra between the rPP and the composites suggests that the introduction of DPF did not significantly alter the chemical composition at the molecular level. Possible factors contributing to this observation include the high compatibility between DPF and the polypropylene matrix, limited chemical changes during the fabrication process, potential dominance of matrix peaks in the FTIR spectra, and minimal disruption of the crystalline structure by well-dispersed DPF. While FTIR provides valuable insights into chemical changes, complementary analyses such as X-ray diffraction or scanning electron microscopy may offer a more comprehensive understanding of structural and morphological aspects, enhancing the interpretation of the observed spectral similarities. The peaks around 3650 cm^{-1} are related to stretching O − H. The strong peaks round 2800–2900 cm^{-1} corresponds to C–H stretching vibrations in cellulose and hemicellulose, as well as rPP. Peak around 1730 cm^{-1} refers to the Carbonyl group (C = O) stretching of hemicellulose. Carbonyl functionality in rPP could be due to degradation and/or ester-based additives (Gall et al., 2021). The band near 1650 cm^{-1} is corresponding to the O − H bending of absorbed water into the cellulose fibers. In rPP, hydroxylic group could be a result of polar contaminants. The peak near 1580 cm^{-1} is representing the aromatic ring C = C of the phenyl propane group such as in lignin. Additional band near 1240 cm^{-1} is attributed to the acetyl group of C − O stretching in hemicellulose, while the band near 1030 cm^{-1} is correspond to the C − O and O − H stretching vibration in cellulose.

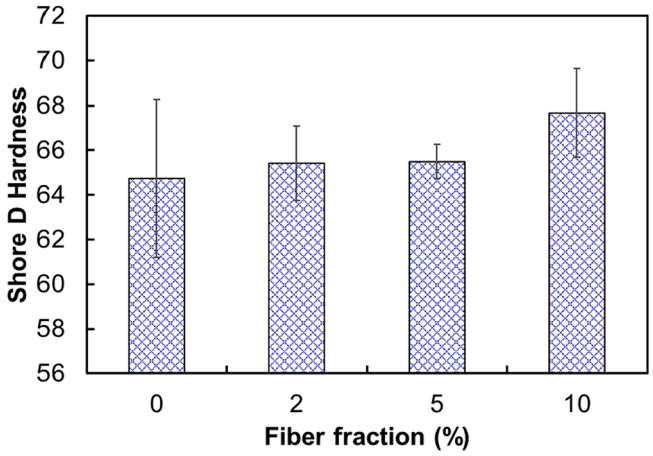

Fig. 6. Effect of fiber fraction on the Shore D hardness of the recycled biocomposites.

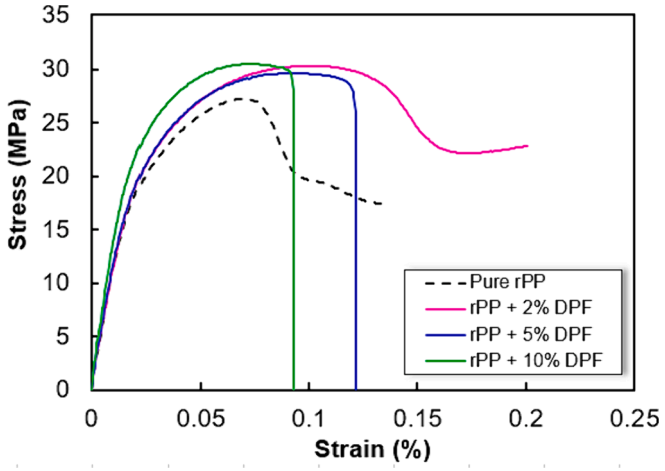

Fig. 7. Tensile stress–strain curves of rPP biocomposite with varying fraction of DPF.

3.3. *Mechanical properties*

The polymer composite needs to be mechanically characterized for their structural applications. We employed Shore D hardness in this understand the effect of fiber content on the hardness of the recycled biocomposites The Shore D hardness increased with the increase in fraction of DPF in the biocomposites and statically higher than the rPP as shown in Fig. 6. The biocomposites with 10 % DPF exhibited the highest hardness of ~ 68 compared to 64.5 in rPP. The slight improvement in hardness values is attributed to the presence of higher volume fraction of DPF which strengthens the rPP matrix. Although the improvement in the composite is not significant compared to rPP, it is interesting that the hardness is not deteriorated by the existence of elastic fibers in the rPP/DPF composite samples. The overall mechanical strength of the composite can be better characterized by the uniaxial tests.

The bulk tensile properties of a polymer can be further improved by reinforcing fibers including natural wood fibers since the latter possess higher mechanical strength compared to polymer matrix. The effect of fiber reinforcement and its content are investigated based on the tensile properties. The room temperature tensile curves of rPP reinforced with varying fraction of DPF is presented in Fig. 7. The UTS of the rPP was found to be ~ 27.3 MPa which is similar to the UTS of neat PP which is

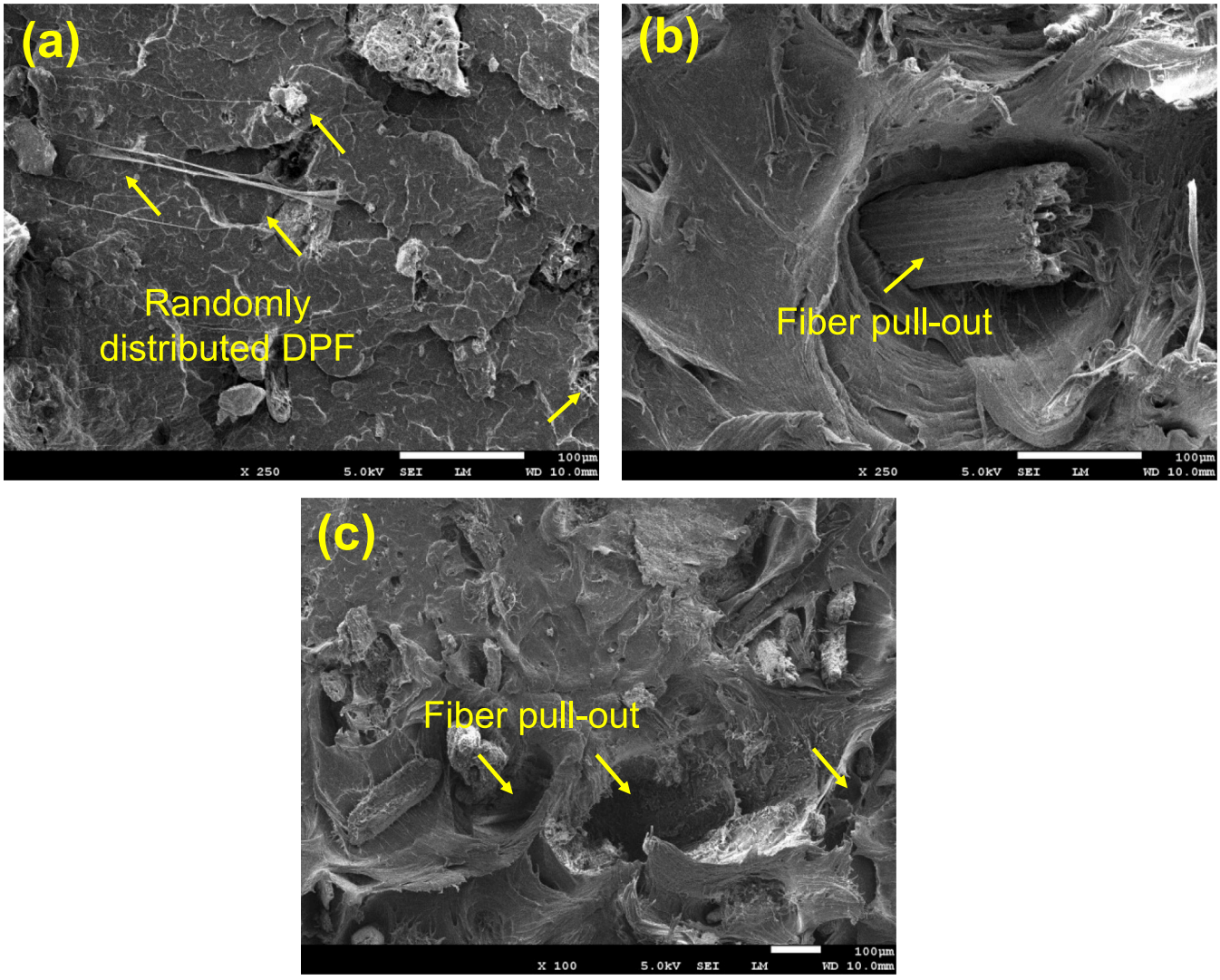

Fig. 8. Fracture behavior and dispersion of DPF in rPP + 10 %DPF biocomposite subjected to tensile loading.

~ 29 MPa (Ku et al., 2011). This confirms that the rPP was free from any impurities and can be a potential candidate to replace neat PP. The tensile strength of the composites increased with the addition of DPF. The UTS was increased by 11.8 % with the addition of 10 % DPF in the rPP. In contrast, the ductility of the composites decreased. The slight decrease in the elongation of the composite with the addition of fibers is attributed to two reasons (i) the fibers were randomly oriented, leading to decrease in stress transfer along the loading direction and (ii) the presence of agglomerated fibers resulting in potential defect sites in the matrix. It must be noted that the tensile properties of biocomposites with 10 % DPF are promising with much higher Young's modulus of 1.36 GPa and tensile strength of ~ 31.9 MPa compared to 1.19 GPa and 27.3 MPa of rPP, respectively. The effectiveness of load transfer can be further improved by aligning the fibers along loading direction and the effect of higher volume fraction of fibers in the matrix will be investigated in future investigations. In general, higher fraction of fibers is recommended in the matrix to achieve high performance composites. However, adding a higher fraction of fibers beyond the percolation limit tends to agglomerate them and deteriorate the mechanical properties. Hence, an optimum fraction of fibers in the matrix needs to be determined. Overall, it is promising that the addition of moderate amount of DPF in the recycled polypropylene can enhance the modulus as well as tensile strength of the biocomposite. Further enhancements can be achieved by chemical treatment of the fibers and aligning the fibers in loading direction.

3.4. Fracture behavior and strengthening mechanism

In order to scrutinize the fiber distribution in the polymer matrix, SEM was performed on the fractured surface. The fractured surface of rPP + 10 % DPF subjected to tensile loading is presented in Fig. 8. The fracture surface in general seems to be irregular and jagged displaying a mixture of slightly brittle and ductile nature of the composite. It is attributed to the presence of randomly oriented DPF. The dispersion of fibers can be seen in Fig. 8(a) where few single strands of DPF can be seen and few agglomerated DPFs can be observed too. It must be noted that the fractured images are presented for rpp + 10 %DPF which is the highest fraction of DPF used in the present study. A typical feature of stress bridging strengthening mechanism can be seen in Fig. 8(b) and (c) where the fiber pull-out mechanism is captured, marked by yellow arrows. The presence of DPF in random fashion and the evident pull-out mechanism contributed towards high tensile strength of the composite compared to its rPP (~27.3 MPa). Better dispersion of the fibers can be achieved by increasing the viscosity of rPP as well as employing dispersion techniques like ultrasonication or vortex mixing during the processing.

4. Conclusions

The utilization of date palm fibers (DPF) as reinforcement in recycled polypropylene (rPP) matrix offers a promising approach for developing sustainable and eco-friendly composite materials. The biocomposite with varying fraction of DPF is successfully fabricated with homogeneous dispersion of DPFs in the rPP matrix. Two step extrusion process further helped in achieving alignment of fibers in the rPP matrix. The thermal degradation temperature increased with the addition of DPF attributed to the lignin content in the DPF. The mechanical characterization of the fabricated composites revealed that the properties, such as hardness and tensile strength, were improved compared to pure recycled polypropylene. This enhancement is attributed to the inherent strength and stiffness of the DPFs, which effectively reinforced the polymer matrix. The strength of the composite can be further improved by chemical treatment of the DPFs which upsurges the surface roughness of DPF ensuing in strong interlocking with the matrix.

CRediT authorship contribution statement

Abdulmohsen Albedah: Writing – original draft, Supervision, Funding acquisition, Resources, Project administration. **Hany S. Abdo:** Writing – review & editing, Visualization, Investigation. **Sohail M.A.K. Mohammed:** Writing – review & editing, Visualization, Data curation. **Bel Abbes Bachir Bouiadjra:** Writing – review & editing, Methodology, Formal analysis. **Ebrahim H. Al-Ghurabi:** Investigation, Formal analysis. **Othman Y. Alothman:** Writing – review & editing, Methodology, Supervision, Resources.

Declaration of competing interest

The authors declare that they have no known competing financial interests or personal relationships that could have appeared to influence the work reported in this paper.

Acknowledgements

The authors extend their appreciation to the Deputyship for Research & Innovation, “Ministry of Education” in Saudi Arabia for funding this research work through the project number (IFKSUDR_P136).

References

Adamu, M., Rehman, K.U., Ibrahim, Y.E., Shatanawi, W., 2023. Predicting the strengths of date fiber reinforced concrete subjected to elevated temperature using artificial neural network, and Weibull distribution. Sci. Rep. 13, 18649. https://doi.org/10.1038/s41598-023-45462-z.

Ahmad, S., Habib, S., Nawaz, M., Shakoor, R.A., Kahraman, R., Tahtamouni, M.A., T.,, 2023. The role of polymeric matrices on the performance of smart self-healing coatings: a review. J. Ind. Eng. Chem. 124, 40–67. https://doi.org/10.1016/J.JIEC.2023.04.024.

Alawar, A., Hamed, A.M., Al-Kaabi, K., 2009. Characterization of treated date palm tree fiber as composite reinforcement. Compos. Part B Eng. 40, 601–606. https://doi.org/10.1016/j.compositesb.2009.04.018.

Ali, A., Shaker, K., Nawab, Y., Jabbar, M., Hussain, T., Militky, J., Baheti, V., 2018. Hydrophobic treatment of natural fibers and their composites—A review. J. Ind. Text. 47, 2153–2183. https://doi.org/10.1177/1528083716654468.

Al-Khanbashi, A., Al-Kaabi, K., Hammami, A., 2005. Date palm fibers as polymeric matrix reinforcement: fiber characterization. Polym. Compos. 26, 486–497. https://doi.org/10.1002/pc.20118.

Al-Otaibi, M.S., Alothman, O.Y., Alrashed, M.M., Anis, A., Naveen, J., Jawaid, M., 2020. Characterization of Date Palm Fiber-Reinforced Different Polypropylene Matrices. Polym. 2020, Vol. 12, Page 597 12, 597. doi: 10.3390/POLYM12030597.

Alzebdeh, K.I., Nassar, M.M.A., Al-Hinai, N., 2021. Development of new eco-composites from natural agro-residues and recycled Polymers. ASME Int. Mech. Eng. Congr. Expo. Proc. 3 https://doi.org/10.1115/IMECE2020-23536.

Bouakkaz, A., Albedah, A., Bouiadjra, B.B., Khan, S.M.A., Benyahia, F., Elmeguenni, M., 2018. Effect of temperature on the mechanical properties of polypropylene–talc composites. J. Thermoplast. Compos. Mater. 31, 896–912. https://doi.org/10.1177/0892705717729016.

Chiang, T.-C., Liu, H.-L., Tsai, L.-C., Jiang, T., Ma, N., Tsai, F.-C., 2020. Improvement of the mechanical property and thermal stability of polypropylene/recycled rubber composite by chemical modification and physical blending. Sci. Rep. 10, 2432. https://doi.org/10.1038/s41598-020-59191-0.

Esmizadeh, E., Tzoganakis, C., Mekonnen, T.H., 2020. Degradation Behavior of Polypropylene during Reprocessing and Its Biocomposites: Thermal and Oxidative Degradation Kinetics. Polym. 2020, Vol. 12, Page 1627 12, 1627. doi: 10.3390/POLYM12081627.

Ferg, E.E., Bolo, L.L., 2013. A correlation between the variable melt flow index and the molecular mass distribution of virgin and recycled polypropylene used in the manufacturing of battery cases. Polym. Test. 32, 1452–1459. https://doi.org/10.1016/j.polymertesting.2013.09.009.

Fouly, A., Abdo, H.S., Seikh, A.H., Alluhydan, K., Alkhammash, H.I., Alnaser, I.A., Abdo, M.S., 2021. Evaluation of Mechanical and Tribological Properties of Corn Cob-Reinforced Epoxy-Based Composites—Theoretical and Experimental Study. Polym. 2021, Vol. 13, Page 4407 13, 4407. doi: 10.3390/POLYM13244407.

Gall, M., Freudenthaler, P.J., Fischer, J., Lang, R.W., 2021. Characterization of composition and structure–property relationships of commercial post-consumer polyethylene and polypropylene recyclates. Polymers (basel). 13, 1574. https://doi.org/10.3390/POLYM13101574/S1.

Gideon, R., Atalie, D., 2022. Mechanical and water absorption properties of jute/palm leaf fiber-reinforced recycled polypropylene hybrid composites. Int. J. Polym. Sci. 2022 https://doi.org/10.1155/2022/4408455.

Quynh Truong Hoang, T., Lagattu, F., Brillaud, J., 2010. Natural fiber-reinforced recycled polypropylene: microstructural and mechanical properties. J. Reinf. Plast. Compos. 29, 209–217. doi: 10.1177/0731684408096931.

Islam, M.R., Beg, M.D.H., Gupta, A., 2014. Characterization of alkali-treated kenaf fibre-reinforced recycled polypropylene composites. J. Thermoplast. Compos. Mater. 27, 909–932. https://doi.org/10.1177/0892705712461511/ASSET/IMAGES/LARGE/10.1177_0892705712461511-FIG16.JPEG.

Ku, H., Wang, H., Pattarachaiyakoop, N., Trada, M., 2011. A review on the tensile properties of natural fiber reinforced polymer composites. Compos. Part B Eng. 42, 856–873. https://doi.org/10.1016/j.compositesb.2011.01.010.

Kusuma, S.S.W., Saputra, H.C., Widiastuti, I., 2021. Manufacturing of natural fiber-reinforced recycled Polymer–a systematic literature review. J. Phys. Conf. Ser. 1808, 012005 https://doi.org/10.1088/1742-6596/1808/1/012005.

Ladhari, A., Kucukpinar, E., Stoll, H., Sängerlaub, S., 2021. Comparison of properties with relevance for the automotive sector in mechanically recycled and virgin polypropylene. Recycling 6, 76. https://doi.org/10.3390/recycling6040076.

Mary Jasmin, N., Sathish, S., Senthil, T.S., Appala Naidu, B., Daniel Das, A., Arun, K.K., Subbiah, R., Srinivasan, K., 2023. Investigation on natural fiber reinforced polymer matrix composite. Mater. Today Proc. 74, 60–63. https://doi.org/10.1016/J.MATPR.2022.11.094.

Mofokeng, J.P., Luyt, A.S., Tábi, T., Kovács, J., 2012. Comparison of injection moulded, natural fibre-reinforced composites with PP and PLA as matrices. J. Thermoplast. Compos. Mater. 25, 927–948. https://doi.org/10.1177/0892705711423291.

Rahimi, A., García, J.M., 2017. Chemical recycling of waste plastics for new materials production. Nat. Rev. Chem. 1, 0046. https://doi.org/10.1038/s41570-017-0046.

Saheb, D.N., Jog, J.P., 1999. Natural fiber polymer composites: a review. Adv. Polym. Technol. 18, 351–363. https://doi.org/10.1002/(SICI)1098-2329(199924)18:4.

Sahu, M., Patnaik, A., Kishor Sharma, Y., Dalai, A., 2023. Physico-mechanical and tribological behaviour of natural fiber reinforced polymer composites: A short review. Mater. Today Proc. doi: 10.1016/J.MATPR.2023.03.822.

Sarmin, S.N., Jawaid, M., Zaki, S.A., Radzi, A.M., Fouad, H., Khiari, R., Rahayu, S., Amini, M.H.M., 2023. Enhancing the properties of date palm fibre reinforced bio-epoxy composites with chitosan – synthesis, mechanical properties, and dimensional stability. J. King Saud Univ. - Sci. 35, 102833 https://doi.org/10.1016/j.jksus.2023.102833.

Sathish, S., Aneesh, S., Naveen Vigneshwaran, S., Nithish Kumar, E.K., Ravichandran, M., Anaz Khan, M., 2023. Role of areca fibres on the mechanical behavior of natural fibre reinforced polymer composite. Mater. Today Proc. doi: 10.1016/J.MATPR.2023.03.606.

Segal, L., Creely, J.J., Martin, A.E., Conrad, C.M., 1959. An empirical method for estimating the degree of crystallinity of native cellulose using the X-ray Diffractometer. Text. Res. J. 29, 786–794. https://doi.org/10.1177/004051755902901003.

Selke, S.E., Wichman, I., 2004. Wood fiber/polyolefin composites. Compos. Part A Appl. Sci. Manuf. 35, 321–326. https://doi.org/10.1016/j.compositesa.2003.09.010.

Shaikh, H., Alothman, O.Y., Alshammari, B.A., Jawaid, M., 2023. Dynamic and thermo-mechanical properties of polypropylene reinforced with date palm nano filler. J. King Saud Univ. - Sci. 35, 102561 https://doi.org/10.1016/j.jksus.2023.102561.

Singh, M.K., Mohanty, A.K., Misra, M., 2023. Upcycling of waste polyolefins in natural fiber and sustainable filler-based biocomposites: a study on recent developments and future perspectives. Compos. Part B Eng. 110852 https://doi.org/10.1016/J.COMPOSITESB.2023.110852.

Zadeh, K.M., Ponnamma, D., Al-Maadeed, A.A.M., 2017. Date palm fibre filled recycled ternary polymer blend composites with enhanced flame retardancy. Polym. Test. 61, 341–348. https://doi.org/10.1016/J.POLYMERTESTING.2017.05.006.